

Dehydrin Genes in Model Brachypodium Grasses

Subjects: [Agronomy](#) | [Evolutionary Biology](#) | [Genetics & Heredity](#)

Contributor: Maria Decena Rodriguez

Dehydration proteins (dehydrins, DHNs) confer tolerance to water-stress deficit in plants. We performed a comparative genomics and evolutionary study of DHN genes in four model *Brachypodium* grass species. Ten dehydrins have been describe within *Brachypodium* species. Due to limited knowledge on dehydrin expression under water deprivation stress in *Brachypodium*, we also performed a drought-induced gene expression analysis in 32 ecotypes of the genus' flagship species *B. distachyon* showing different hydric requirements. Bdhn1 - Bdhn2, Bdhn3 and Bdhn7 genes, orthologs of wheat, barley, rice, sorghum, and maize genes, were more highly expressed in plants under drought conditions.

Bdhn genes

cis-regulatory elements

comparative genomics

dehydrin structure

dehydrin-gene expression

duplicated genes

drought-related traits

drought-tolerant ecotypes

phylogenetics

1. Introduction

Water deprivation is one of the main abiotic stresses that affect plant development and fitness ^{[1][2]}. Water deficit stress in plants is mostly caused by low soil water content but also by other abiotic stresses such as salinity and extreme temperature ^{[3][4]}—which sometimes interact ^[2]—affecting the survival of plants in a wide range of environmental conditions ^{[4][5]}. Plant species adapted to dry environments have developed mechanisms to protect their cells from water stress deficit. Among the several physiological and genomic regulatory mechanisms triggered by water limitation in plants, there is an almost universal response in the upregulation of dehydrins ^{[1][4][6]}. Dehydrins (DHN) belong to group 2 LEA (Late-Embryogenesis-Abundant) proteins ^[7], and are intrinsically disordered hydrophilic proteins that acquire structure when bound to ligands, such as membranes, acting as chaperones that impede the aggregation or inactivation of other proteins under desiccation to maintain the biological activity of the cell ^{[8][9]}. They show a high hydration capacity and can also bind large quantities of cations, retaining water in the drying cells and preventing ionic unbalance and protein denaturation. DHNs are also called RAB proteins because they are usually responsive to abscisic acid ^[9]. DHNs accumulate in all vegetative tissues under water stress, though with different specificities ^[4], as well as during seed development ^[8].

The dehydrin protein family is characterized by a modular sequence domain (Dehydrin) that contains three conserved segments (Y, S, K; ^{[8][10]}; **Figure 1a**). The dehydrin identifier K-segment motif is present in all plant

DHNs except for HIRD11 (see [Section 2](#)). Perdiguero et al. demonstrated the induction of dehydrin genes lacking the K-segment under drought stress in *Pinus* [\[11\]](#). The S-segment is located between the Y and K segments and, when phosphorylated, transfers dehydrins and other nuclear localization signal (NLS) binding proteins from the cytosol to the nucleus [\[10\]\[12\]](#). The Y-segment motif is located towards the N-terminus of the protein coding region. The Y, S, and K segments are interspersed by other less conserved segments, named interpattern or ϕ -segments that mostly contain small, polar, and charged amino acids [\[13\]](#). Recent studies have described another conserved F-segment motif in some seed plant DHNs [\[11\]\[14\]](#). This segment, when present, has a unique copy and is located between the N-terminus of the protein coding region and the S-segment. An additional NLS-segment motif was found in some dehydrin families of maize [\[12\]](#). Different combinations of conserved motifs have been used to classify the dehydrin domain into major architectures, with five of them (K_n , SK_n , K_nS , Y_nK_n , Y_nSK_n) being common across angiosperms [\[10\]](#). The dehydrin domain is occasionally fused with upstream DNAJ-X and DNA-J containing gene domains in some DHN genes [\[10\]](#). DNA-J is a heat shock protein (Hsp40) that prevents the aggregation of unfolded proteins and functions as a chaperone folding protein when associated with Hsp70 under water-stress [\[10\]\[15\]](#) (**Figure 1a**). Evolutionary studies of spermatophyte dehydrins identified Kn or SKn as the oldest ancestral architectures whereas those containing the Y segment arose only in the angiosperms [\[10\]\[16\]](#). Two main architectural changes apparently occurred after the ancestral whole genome duplication events of the angiosperms, the Y3SK2-Y3K1 and Y1SK2-K6 dehydrins [\[10\]](#). Whereas K6 developed a novel function in cold protection (but see [\[16\]](#) for the important role of Kn dehydrins in drought protection), Y3K1 showed signatures of pseudogenization in some families (e.g., the Brassicaceae) [\[10\]](#). At the infrageneric level, the dehydrin phylogeny of 11 *Oryza* species showed the splits of four high-to-weakly supported domain clades and a lack of dehydrin-specific subclades [\[9\]](#).

DHNs have been extensively studied in grasses due to their key role as agents conferring water-stress tolerance in cereal and forage crops [\[7\]\[9\]\[17\]\[18\]](#). Expression of dehydrins under drought stress has been positively associated with plant biomass and grain yield [\[19\]](#). Several in vitro studies have demonstrated that DHN expression enhances plant stress tolerance [\[20\]\[21\]](#). Dehydrins maintain the osmotic balance of cells and their chlorophyll contents, bind metals to scavenge ROS, and bind to DNA and phospholipids [\[20\]\[22\]](#). Despite these advances, some of the biological functions of DHNs have not been fully established yet [\[10\]](#). Few dehydrins have been characterized biochemically, like those involved in enzyme and membrane bioprotection in *Triticum* [\[23\]](#) and *Zea* [\[24\]](#) and in protection against ROS in *Arabidopsis* and *Brassica* [\[25\]\[26\]](#). Their protective activities have been experimentally demonstrated in some cases using circular dichroism (e.g., *Zea mays* DHN1 binding to lipid vesicles, [\[27\]](#); *Hordeum vulgare* Dhn5 protection of lactate dehydrogenase under drought and cold conditions, [\[28\]](#)).

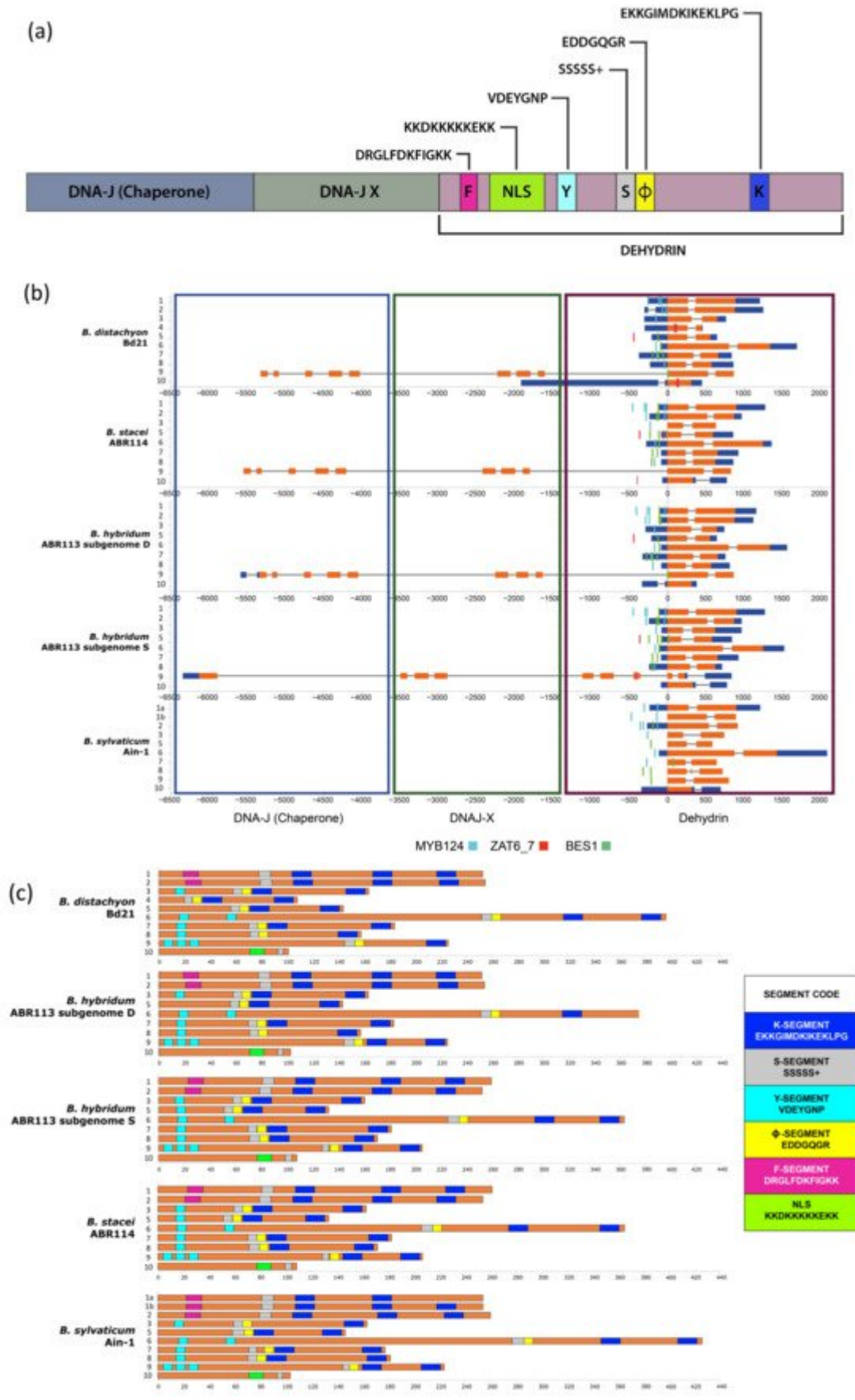


Figure 1. Schematic structure of a typical grass DHN gene showing the positions of the main domains and coding segments (a). Gene structure of *Brachypodium distachyon* Bd21, *B. stacei* ABR114, *B. hybridum* ABR113 (D and S subgenomes), and *B. sylvaticum* Ain-1 dehydrins showing: (b) the three detected DNA J (purple rectangle), DNA J-X (light green rectangle) and dehydrin (dark green rectangle) domains, and their CDSs (orange bars), introns (grey lines), and 5' and 3' UTRs (blue bars); (c) the conserved motifs of their CDSs with their respective K (dark blue), S (grey), Y (light blue), ϕ (yellow), F (pink), and NLS (light green) segments. *Brachypodium* dehydrin gene codes (*Bdhn1–Bdhn10*) correspond to those indicated in **Table 1**. *Cis*-regulatory elements BES1, MYB124, and ZAT are mapped in the promoters of each gene (see color codes in the chart; the figure could be also visualized in http://zeta.uma.es/public/journal/brachy/DHN_Brachy_4_varieties.html, 29 November 2021).

Table 1. Dehydrin genes found in the studied *Brachypodium distachyon*, *B. stacei*, *B. hybridum* (subgenomes D and S), and *B. sylvaticum* species. *Brachypodium* dehydrin gene codes (*Bdhn1–Bdhn10*) given in this study, the protein structure and their corresponding Panther family and subfamilies gene codes. Phytozome dehydrin gene codes correspond to the respective gene numbers in the reference genome of each species deposited in Phytozome.

<i>Bdhn</i>	Structure	Panther Family	Panther Subfamily	Phytozome Dehydrin Gene Codes				
				<i>B. distachyon</i> (Bd21)	<i>B. stacei</i> (ABR114)	<i>B. hybridum</i> D (ABR113)	<i>B. hybridum</i> S (ABR113)	<i>B. sylvaticum</i> (Ain1)
<i>Bdhn1a</i>				Bradi5g10860	Brast09G089800	Brahy.D05G0138300	Brahy.S09G0091400	Brasy9G143400
<i>Bdhn1b</i>	FSK _n		ERD14					Brasy9G149400
<i>Bdhn2</i>	FSK _n			Bradi3g51200	Brast04G110500	Brahy.D03G0707100	Brahy.S04G0117200	Brasy4G117200
<i>Bdhn3</i>	Y _n SK _n		SF23	Bradi1g37410	Brast07G152200	Brahy.D01G0507100	Brahy.S07G0169500	Brasy7G144000
<i>Bdhn4</i>	Y _n SK _n	PTH33346	SF14	Bradi4g22280				
<i>Bdhn5</i>	Y _n SK _n			Bradi4g22290	Brast05G049400	Brahy.D04G0319400	Brahy.S05G0054400	Brasy5G271500
<i>Bdhn6</i>	Y _n SK _n		SF 19	Bradi4g19525	Brast05G075400	Brahy.D04G0277700	Brahy.S05G0083200	Brasy4G237500
<i>Bdhn7</i>	Y _n SK _n		SF14	Bradi3g43870	Brast04G194300	Brahy.D03G0604200	Brahy.S04G0208500	Brasy4G220100
<i>Bdhn8</i>	Y _n SK _n			Bradi3g43855	Brast04G197200	Brahy.D03G0604000	Brahy.S04G0208900	Brasy4G219800
<i>Bdhn9</i>	Y _n SK _n		XERO I	Bradi2g47575	Brast01G171900	Brahy.D02G0637300	Brahy.S01G0182800	Brasy1G228900
<i>Bdhn10</i>	K*NLSL-S	PTHR34941	HIRD 11	Bradi1g13330	Brast02G251900	Brahy.D01G017200	Brahy.S02G0268100	Brasy2G277500

genus have been selected as a model complex for polyploidy (diploids *B. distachyon* and *B. stacei* and derived allotetraploid *B. hybridum*; [30]) and one of its perennial species has been selected as a model species for perenniality (diploid *B. sylvaticum*; [31]). Transgenic plants of its flagship species *B. distachyon* have been analyzed to identify candidate genes that enhance drought stress tolerance in plants [32][33][34] though none of them specifically addressed dehydrins. Inspection of an early version of the *B. distachyon* reference genome Bd21 detected 36 LEA2 encoding genes but did not characterize the dehydrin genes [35]. The dehydrin gene content, structure, evolution, and expression in response to drought among species and accessions of *Brachypodium* has not been investigated yet.

Given the significance of DHNs in water stress response of grasses, we analyzed the members of the dehydrin gene family in the four *Brachypodium* model species and in 54 *B. distachyon* ecotypes showing different hydric requirements and drought tolerances using in silico analysis of genome annotations. Due to the lack of studies on dehydrin expression under water deprivation stress in *Brachypodium* we also performed DHN expression analysis in 32 *B. distachyon* ecotypes under different drought and watered conditions. The aims of our study were: (i) to identify and characterize the *Brachypodium* dehydrin genes (*Bdhn*) and the structure and biochemical properties of the encoded proteins, comparing them with those of the closely related cereal crops (*Hordeum*, *Oryza*, *Sorghum*, *Triticum-Aegilops*, *Zea*), and to evaluate the presence of enriched sequence motifs that may have potential regulatory effects (ii) to analyze the syntenic distributions and origins of the *Bdhn* genes, identify gene duplication events, and test the functionality of paralogs, (iii) to investigate their expression profiles under control vs. dry conditions and compare them to those of closely related cereals, and (iv) to correlate the dehydrin gene expressions with the phenotypic and environmental traits of the plants and test their potential phylogenetic signal.

2. Dehydrin Genes of *Brachypodium* Species and Outgroup Grasses

Genome searches in Phytozome and Ensembl Plants retrieved 47 dehydrin gene sequences collected from the reference genomes of the four sequenced *Brachypodium* species [*B. distachyon* Bd21 $2n = 2x = 10$, $x = 5$ (10); *B. sylvaticum* Ain-1 $2n = 2x = 18$, $x = 9$ (10); *B. stacei* ABR114 $2n = 2x = 20$, $x = 10$ (9); *B. hybridum* ABR113 $2n = 4x = 30$, $x = 5 + 10$ (18; 9 from its *B. distachyon*-type D subgenome and 9 from its *B. stacei*-type S subgenome)] (**Table 1; Figure 1b**). A total of 54 orthologous DHN sequences were retrieved from the reference genomes of six outgroup grass species [*Aegilops tauschii* $2n = 2x = 14$, $x = 7$ (9); *Hordeum vulgare* $2n = 2x = 14$, $x = 7$ (8); *Zea mays* $2n = 2x = 20$, $x = 10$ (7); *Oryza sativa* $2n = 2x = 24$, $x = 12$ (6); *Sorghum bicolor* $2n = 2x = 20$, $x = 10$ (5); *Triticum aestivum* $2n = 6x = 42$, $x = 7$ (19); [Supplementary Table S1](#)]. A new nomenclature was created for the *Brachypodium* dehydrin genes (*Bdhn1* to *Bdhn10*; **Table 1; Figure 1b,c**). In several instances we used the same numbers as those of the orthologous *Hordeum vulgare* DHN genes (*Bdhn* 6-7, and *Bdhn* 9-10) (ENA database: AF043086, AF043092; AF043086 and Genbank database: AY681974) and the orthologous *Oryza sativa* DHN genes (*Bdhn1-2* and *Bdhn8*) (RAP database: Os02g0669100, Os11g0454300). *Bdhn3* was numbered according to prior annotation in *Brachypodium* (GeneBank: XM_010229280), whereas the remaining *Bdhn* genes were numbered consecutively as *Bdhn4* and *Bdhn5*. The *Bdhn* genes were also classified according to Panther protein gene families (PTH33346 and PTH34941) and subfamilies (ERD14, XERO1, SF14, SF19, SF23, HIRD11; **Table 1**). All *Bdhn10* genes found in the studied species of *Brachypodium* lacked the K-segment (**Figure 1c**). However, those dehydrins showed an extraordinary sequence identity with typical DHNs, including those with a modified K-segment, like DHN-13 from *H. vulgare* [36]. The absence of the K-segment has been also reported in one dehydrin of pine species [11] and four dehydrins of rice species (OnDHN6, OrDHN7, OIDHN3, OIDHN6; [9]). These *Brachypodium* *Bdhn10* dehydrins, with architecture K*(NLS)S, belong to HIRD11 proteins and show orthology with DHN genes from *H. vulgare*, *O. sativa*, *S. bicolor*, and *Z. mays* ([Supplementary Table S1](#)).

The *Brachypodium* dehydrins showed different lengths, ranging from 86.3 (*Bdhn10*) to 323 amino acid residues (*Bdhn6*), molecular weights from 9762.90 to 30945.54 kDa, and isoelectric points from 4.41 (*Bdhn2*) to 7.6 (*Bdhn7*) (9.4 (*Bdhn4*) in *B. distachyon*) ([Supplementary Table S2](#)). All dehydrins presented a negative GRAVY value, indicating that they are hydrophilic proteins. All *Bdhn* genes except *Bdhn5* were structurally conserved across the four *Brachypodium* species (**Figure 1b,c**). *Bdhn4* was only present in *B. distachyon*, while *Bdhn1* was duplicated in *B. sylvaticum* (*Bdhn1a*, *Bdhn1b*) (**Table 1**; **Figure 1b,c**). All *Bdhn* genes but *Bdhn9* showed a single dehydrin domain. *Bdhn9* encoded a protein of 508 aa with DHN–DNAJ–X–DNA–J domains in all species except in *B. sylvaticum*, which showed a gene consisting only of the DHN domain (222 aa) ([Supplementary Table S2](#); **Figure 1b**). Eight gene architectures were found along the *Bdhn1*–*Bdhn10* genes (FSK₂, FSK₃, S ϕ K₂, YS ϕ K₂, YS ϕ K, Y₃S ϕ K, Y₃S ϕ K₂, NLS–K*S), with YS ϕ K₂ being the most common architecture present in four genes (*Bdhn3*, *Bdhn6*, *Bdhn7*, *Bdhn8*; **Table 1**, **Figure 1c**). *Bdhn* 3D modeling indicated that the disordered *Brachypodium* dehydrins lacked tertiary structure whereas their secondary structure consisted of different numbers of α -helices (1–4) and β -sheets in some inferred proteins ([Supplementary Figure S1](#)).

Orthology analysis indicates that *Bdhn* genes were also present in the other surveyed grasses. In total, 6 out of 10 *Bdhn* genes were found in *A. tauschii*; *Bdhn1-2* copies were also present in *H. vulgare* and *T. aestivum*, *Bdhn3* in *T. aestivum*, *Bdhn4-5* in *H. vulgare*, *Bdhn7-8* in *T. aestivum*, *Bdhn9* in *O. sativa* and *S. bicolor*, and *Bdhn10* in *H. vulgare*, *O. sativa*, *S. bicolor*, and *Z. mays* ([Supplementary Table S1](#)). By contrast, five DHN genes of *O. sativa* (Os01g0702500, Os11g0453900, Os01g0624400, Os01g0225600, Os03g0655400), four of *H. vulgare* (HORVU6Hr1G083960, HORVU6Hr1G011050, HORVU5Hr1G103460, HORVU3Hr1G089300), and three of *Z. mays* (Zm00001d017547, Zm00001d043730, Zm00001d013647) had no orthologous sequences in *Brachypodium*. Pairwise amino acid sequence similarities indicated that *Bdhn4* and *Bdhn5* were the most similar proteins, followed by *Bdhn1* and *Bdhn2*. *Bdhn10* was the most dissimilar dehydrin. Dehydrins with YS ϕ K₂ structure were in general similar to each other both in *Brachypodium* and in the other grasses.

3. Cis-Regulatory Elements of *Bdhn* Genes

We performed de novo discovery analysis of *cis*-regulatory elements (CREs) of *Bdhn* genes, searching for binding sites of transcription factors (TF) that accumulate around the transcriptional start site and that may control gene expression ([Supplementary Figure S2](#)). The analysis consistently identified three clusters, BES1/BZR1, MYB124, and ZAT binding sites (**Table 2**; [Supplementary Figure S2a](#)) that are related with different drought-response signaling pathways. BES1/BZR1 and MYB124 motifs were present in all studied promoters, though MYB124 was predominant in the promoters of *Bdhn1* and *Bdhn2* and BES1/BZR1 in those of *Bdhn7* genes and more abundantly in those of the aridic *B. stacei* and *B. hybridum* species. By contrast, ZAT was only found in the promoters of *Bdhn4*, *Bdhn5*, and *Bdhn10* genes in annual species (**Table 2**; [Supplementary Figure S2a](#)).

Table 2. Upstream putative *cis*-regulatory elements (CREs) found in the promoter region (–500-to+200 bp) of the *Bdhn* genes of *Brachypodium distachyon*, *B. stacei*, *B. hybridum* (subgenomes D and S), and *B. sylvaticum* using Rsat::plants tools and the corresponding reference genome as background. Family identification, motif code (ID), N-cor (normalized correlation), and Sig (significance value) for the highest hit, matches to

transcription factor (TF) binding sites, and *Bdhn* genes with the number of sites found within each species and gene. Species and reference genomes: BD, *B. distachyon* Bd21; BS, *B. stacei* ABR114; BHD, *B. hybridum* subgenome D ABR113; BHS, *B. hybridum* subgenome S ABR113; BS, *B. sylvaticum* Ain1. Mapping positions of these *cis*-regulatory motifs are indicated in **Figure 1b**.

Family ID	Motif ID	Ncor	Sig	TF Binding Site	<i>Bdhn</i> Genes (No. Sites Found)
BRI1-EMS suppressor/brassinazole-resistant	BES1/BZR1	0.719	4.08		BD: <i>Bdhn</i> 5(1) <i>Bdhn</i> 6(1) <i>Bdhn</i> 7(3) <i>Bdhn</i> 9(1)
					BHD: <i>Bdhn</i> 1(1) <i>Bdhn</i> 2(2) <i>Bdhn</i> 5(1) <i>Bdhn</i> 6(1) <i>Bdhn</i> 7(3) <i>Bdhn</i> 9(1)
					BHS: <i>Bdhn</i> 1(1) <i>Bdhn</i> 2(2) <i>Bdhn</i> 5(4) <i>Bdhn</i> 6(1) <i>Bdhn</i> 7(2) <i>Bdhn</i> 8(1)
					BS: <i>Bdhn</i> 1(1) <i>Bdhn</i> 2(2) <i>Bdhn</i> 5(3) <i>Bdhn</i> 6(1) <i>Bdhn</i> 7(2) <i>Bdhn</i> 8(1)
					BSY: <i>Bdhn</i> 2(1) <i>Bdhn</i> 5(1) <i>Bdhn</i> 7(1) <i>Bdhn</i> 8(2) <i>Bdhn</i> 9(1)
Myb	MYB124	0.598	2.18		BD: <i>Bdhn</i> 1(5) <i>Bdhn</i> 2(4) <i>Bdhn</i> 3(2) <i>Bdhn</i> 6(1) <i>Bdhn</i> 7(2) <i>Bdhn</i> 8(2)
					BHD: <i>Bdhn</i> 1(7) <i>Bdhn</i> 2(4) <i>Bdhn</i> 3(2) <i>Bdhn</i> 6(1) <i>Bdhn</i> 7(2) <i>Bdhn</i> 8(2)
					BHS: <i>Bdhn</i> 1(7) <i>Bdhn</i> 2(4) <i>Bdhn</i> 3(2) <i>Bdhn</i> 6(1) <i>Bdhn</i> 8(2)
					BS: <i>Bdhn</i> 1(8) <i>Bdhn</i> 2(4) <i>Bdhn</i> 3(2) <i>Bdhn</i> 6(1) <i>Bdhn</i> 8(2)
					BSY: <i>Bdhn</i> 1a(4) <i>Bdhn</i> 1b(4) <i>Bdhn</i> 2(4) <i>Bdhn</i> 3(2) <i>Bdhn</i> 6(1) <i>Bdhn</i> 7(2)
C2H2 zinc finger	ZAT	0.738	4.91		BD: <i>Bdhn</i> 4(3) <i>Bdhn</i> 5(1) <i>Bdhn</i> 10(2)
					BHD: <i>Bdhn</i> 5(1)
					BHS: <i>Bdhn</i> 5(1) <i>Bdhn</i> 10(1)
					BS: <i>Bdhn</i> 5(2) <i>Bdhn</i> 10(1)

clade from the rest, followed by the isolated *Bdhn10* (ERD11) clade. Within the remaining group of Y_nSK_n dehydrin structural genes, there was a divergence of the *Bdhn9* (XERO1) clade, followed by subsequent divergences of the Y_nSK_n *Bdhn4*-*Bdhn5*, *Bdhn6*, *Bdhn3*, and *Bdhn7*/*Bdhn8* clades (**Figure 2**). All *Bdhn* clades were monophyletic except the paraphyletic *Bdhn9* and *Bdhn10* clades, which included orthologous sequences from closely related outgroups. Intra-clade branches were overall well-supported except for the poorly informative *Bdhn10* clade.

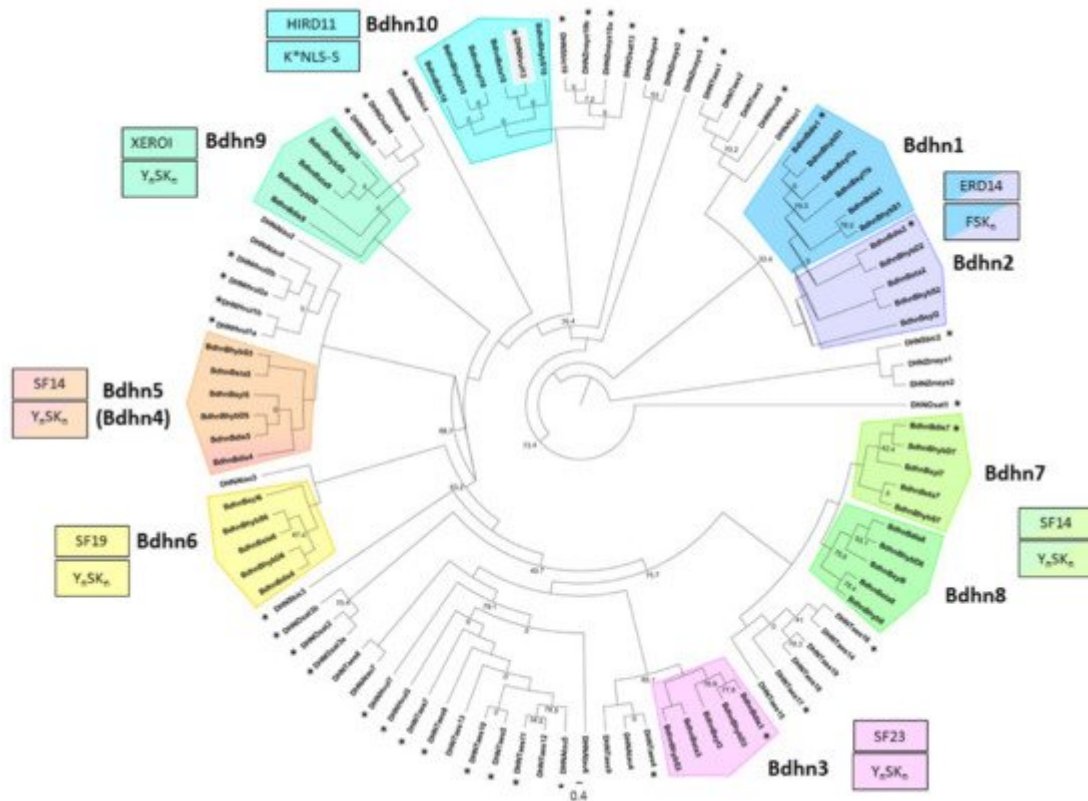


Figure 2. Maximum likelihood *Brachypodium Bdhn* tree. Unrooted IQtree cladogram showing the relationships among the dehydrin *Bdhn* gene clades and orthologous grass sequences (Atau: *Aegilops tauchii*; Hvul: *Hordeum vulgare*; Osat: *Oryza sativa*; Sbic: *Sorghum bicolor*; Taes: *Triticum aestivum*; Zmays: *Zea mays*) and among *Brachypodium* species and genomes within each clade. *Bdhn* clades are identified by colors, *Bdhn* codes, gene architecture, and Panther subfamily codes (see **Table 1**). Duplicated *Bdhn* genes form sister clades or fall within the same clade. Ultrafast bootstrap support (<80%) is shown on branches; the remaining branches are fully supported. Asterisks indicate dehydrin genes differentially expressed under drought vs. control conditions (see text and [Supplementary Table S10](#)). Scale bar: number of mutations per site.

5. Chromosome Distributions and Selection Analysis of Duplicated *Bdhn* Genes

We analyzed the physical distributions of *Bdhn* genes on the chromosomes of the studied species to detect the potential occurrence of tandem or segmental duplication. We also performed selection tests on the coding regions of the *Bdhn* genes to explore the potential loss of selective constraints on them. Dehydrin genes were distributed among the five chromosomes of *B. distachyon* Bd21 and the D subgenome of *B. hybridum* ABR113 (Bd), in 6 out of 10 chromosomes of *B. stacei* ABR114 and the S subgenome of *B. hybridum* ABR113 (Bs), and in 6 out of 9 chromosomes of *B. sylvaticum* Ain-1 (Bsy) (**Figure 3**, [Supplementary Table S3](#)). We detected four tandem duplications and two segmental duplications of *Bdhn* genes. In *B. distachyon* and *B. hybridum* D subgenome our analysis detected tandem duplications of *Bdhn7-Bdhn8* in Bd3 and of *Bdhn4-Bdhn5* in Bd4 (only *B. distachyon*), and a segmental duplication of *Bdhn1-Bdhn2* in Bd3 and Bd5 (**Figure 3**, [Supplementary Table S3](#)). *B. stacei* and *B.*

hybridum S subgenome and *B. sylvaticum* showed a tandem duplication of *Bdhn7-Bdhn8* in Bs4 and Bsy4, and a segmental duplication of *Bdhn1-Bdhn2* in Bs4 and Bs9 and in Bsy4 and Bsy9, respectively. In addition, *B. sylvaticum* showed a tandem duplication of *Bdhn1a* and *Bdhn1b* in Bsy9 not found in the other *Brachypodium* species studied (**Figure 3**, [Supplementary Table S3](#)). Overall, all the selection tests performed with branch-sites models (aBSREL (adaptive Branch-Site Random Effects Likelihood) and BUSTED (Branch-Site Unrestricted Statistical Test for Episodic Diversification) for internal branches only and for leaf branches only) failed to detect evidence of positive selection in all the *Bdhn* genes and species all (p -values >0.05) except for two significant cases. aBSREL tests for internal branches only detected evidence of positive selection in *Bdhn6* and *Bdhn10* (one branch each) where ω_2 rate class values were >1 but for very low percentages of tree branches (*Bdhn6*: $p = 0.04$, $\omega_1 = 0.140$ (97%), $\omega_2 = 53.9$ (2.6%); *Bdhn10*: $p = 0.02$, $\omega_1 = 0.0$ (99%), $\omega_2 = 100,000$ (1.1%); [Supplementary Materials S1](#)). Whereas aBSREL tests for positive selection modeling both site-level and branch-level ω heterogeneity, BUSTED performs a gene-wide (and not site-specific) test for positive selection. Similarly, selection tests performed at sites [MEME (Mixed Effects Model of Evolution)] did not detect evidence of positive selection at any site across the sequences of the *Bdhn* genes except for two significant or marginally significant positions in genes *Bdhn1-Bdhn2* (site 139, $p = 0.04$; site 163, $p = 0.02$) and two in *Bdhn6* (site 266, $p = 0.04$; site 412, $p = 0.05$) ([Supplementary Materials S1](#)). The greater power of MEME indicates that selection acting at individual sites is considerably more widespread than constant models would suggest. It also suggests that natural selection is predominantly episodic, with transient periods of adaptive evolution masked by the prevalence of purifying or neutral selection on other branches.

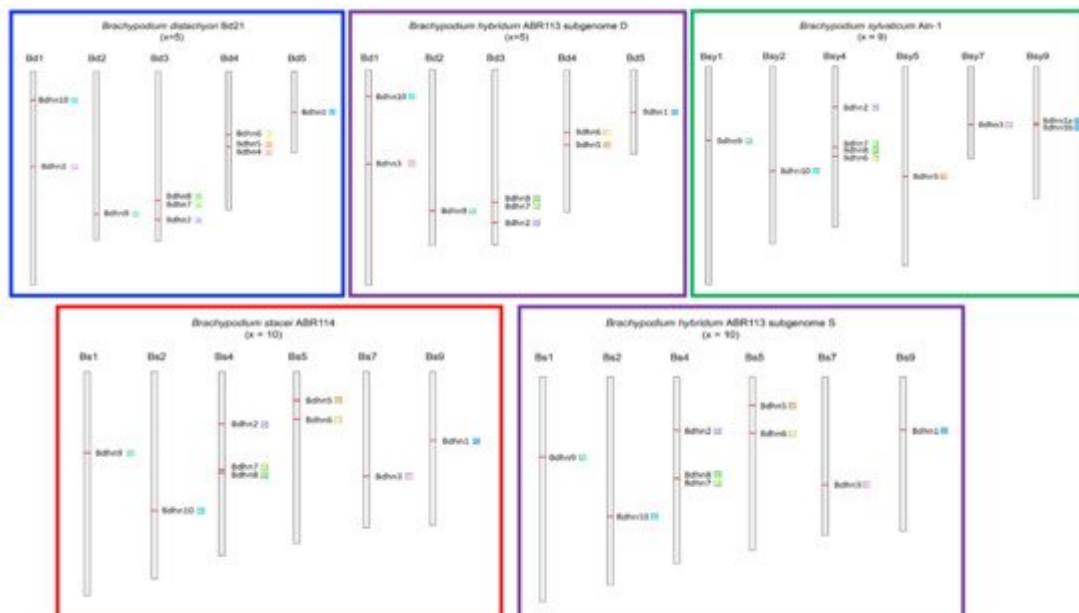


Figure 3. Chromosomal location of *Bdhn* genes in the studied *Brachypodium* species. *B. distachyon* (blue rectangle), *B. stacei* (red), *B. hybridum* subgenomes S and D (purple), and *B. sylvaticum* (green). *Bdhn* genes are mapped on the chromosome with their respective color flags (see **Figure 2**).

6. Dehydrin Gene Clusters, Phylogenetics, and Climate Niche Variation in *B. distachyon*

The genomes of 54 *B. distachyon* ecotypes distributed across the Mediterranean region ([Supplementary Table S4](#)) were annotated for the 10 *Bdhn* gene clusters for comparative genomics, evolutionary, and phylogenetic signal of drought-related traits and climate niche analyses. Most ecotypes (74.07%) contained all 10 *Bdhn* genes ([Supplementary Figure S3](#)) and were used for downstream analyses. Independent ML trees obtained for each separate *Bdhn* gene, based on exon and intron sequences, showed differently resolved topologies ([Supplementary Figure S4](#)). Six of those 10 gene trees (*Bdhn1*, *Bdhn2*, *Bdhn3*, *Bdhn6*, *Bdhn7*, *Bdhn8*) recovered a congruent topology for some *B. distachyon* groups. A ML tree constructed from their concatenated sequences produced a single combined *B. distachyon* *Bdhn* tree (**Figure 4a**) showing a resolution similar to those observed previously in the *B. distachyon* nuclear-SNPs [\[37\]](#) (**Figure 4b**) and plastome [\[38\]](#) (**Figure 4c**) trees. The *Bdhn* tree revealed a relatively well-supported EDF+ clade (74% BS) and the successive but weakly supported divergences of the S+ and T+ lineages, with a clade of T+ lineages (Bd18-1, Bd21-3, BdTR5i) resolved as sister to the EDF+ clade (**Figure 4a**). Topological congruence Kishino-Hasekawa (KH), Shimodaira-Hasekawa (SH), and Shimodaira Approximately Unbiased (AU) tests performed between the *B. distachyon* *Bdhn* tree and the nuclear-SNP and plastome trees indicated that the topology of the *Bdhn* tree did not significantly differ ($p < 0.001$) from the topologies of the two compared trees ([Supplementary Table S5](#)), indicating that all three data sets recover congruent evolutionary histories for the divergences of the main *B. distachyon* lineages. However, the *Bdhn* tree visually resembled more the plastome tree than the nuclear tree (**Figure 4**).

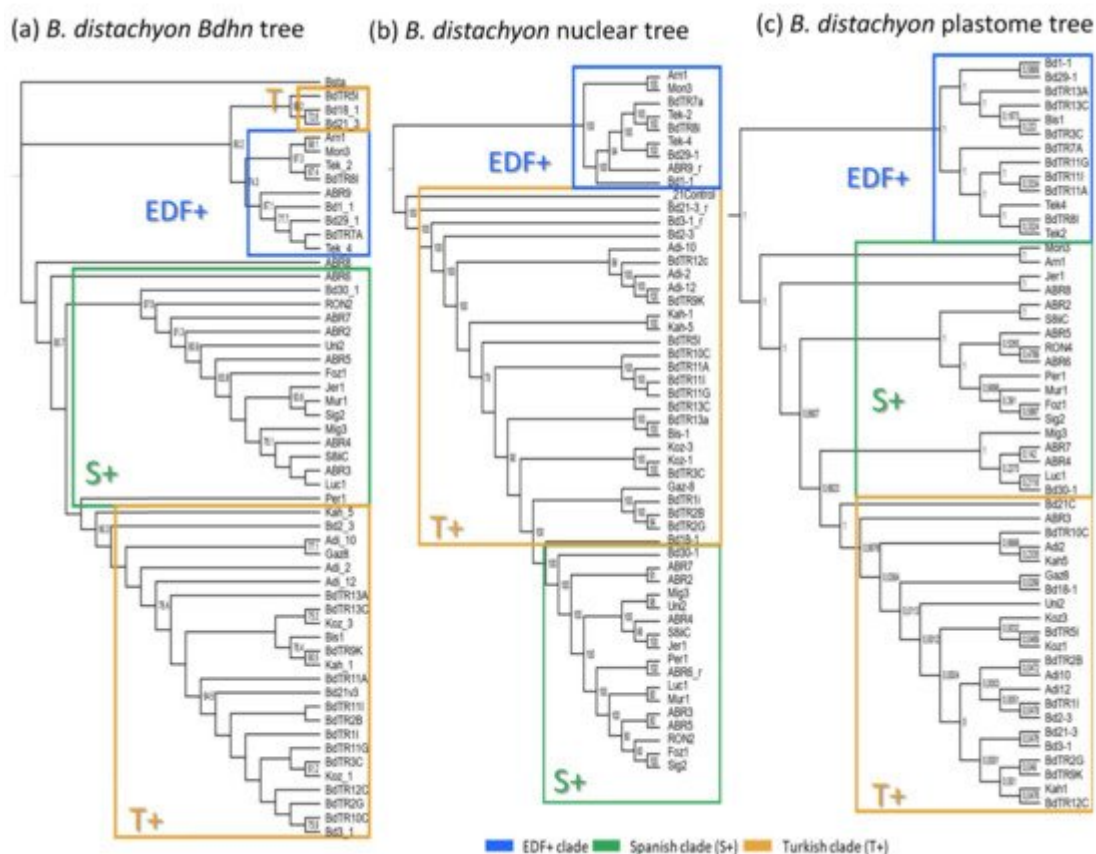


Figure 4. (a) Maximum likelihood *B. distachyon* *Bdhn* tree. Consensus tree constructed for 54 *B. distachyon* ecotypes from concatenated exon and intron aligned sequences of six dehydrin genes (*Bdhn1*, *Bdhn2*, *Bdhn3*, *Bdhn6*, *Bdhn7*, and *Bdhn8*). The EDF+ (extremely delayed flowering time, blue) clade, T+ (Turkish and East Mediterranean, orange), and S+ (Spain and West Mediterranean, green) lineages correspond to those indicated in [37][38]. Bootstrap support is indicated on branches. Accession codes correspond to those indicated in [Supplementary Table S4](#). (b) *B. distachyon* nuclear species tree of [37] based on nuclear genome-wide 3.9 million SNPs. (c) *B. distachyon* plastome tree of [38] based on full plastome sequences.

Climate niches were constructed for the studied *B. distachyon* ecotypes to explore if they present differences in climate niche parameters that could be related to distinct responses to drought. The optimal climate niche of each *B. distachyon* ecotype was inferred from PCA of 19 climate variables ([Supplementary Table S6 and Figure S5](#)). The main PC1 axis (51.8% of variance) values allowed us to classify the *B. distachyon* ecotypes into cold (>2.5; ABR2, ABR3, ABR4, ABR5, ABR6, RON2), warm (<2.5; Bd2-3, Bd21, Bd3-1, Bis1, Kah1, Kah5, Koz1, Koz3), and mesic (-2.5 to 2.5, remaining) climate class ecotypes.

7. Differential Expression of *Bdhn* Genes in *Brachypodium distachyon* Ecotypes under Drought and Temperature Stress Conditions

We made use of data from an extensive transcriptome study of 32 *B. distachyon* ecotypes [39], which enabled us to explore intraspecific variation in how *Bdhn* genes are expressed in response to drought in mature plants. Development and tissue specific expression analysis of dehydrin genes was performed in 32 out of the 54 genomically sequenced ecotypes of *B. distachyon* ([Supplementary Table S4](#)). Only 4 out of the 10 identified *Bdhn* genes were expressed in mature leaves of all 32 studied *B. distachyon* ecotypes: *Bdhn1a* (Bradi5g10860.1), *Bdhn2* (Bradi3g51200.1), *Bdhn3* (Bradi1g37410.1), *Bdhn7* (Bradi3g43870.1); [Supplementary Table S7](#). These annotated dehydrins showed significant differential expression (DE) levels between the watered (W) and dry (D) conditions, independently of temperature conditions in both separate CD-CW-HD-HW and averaged D vs. W comparative tests ([Supplementary Table S8 and Figure S6a,b](#)). By contrast, the dehydrin expressions did not show significant differences between cool (C) and hot (H) conditions under drought treatment, and only *Bdhn3* and *Bdhn7* showed significant differences in CW vs. HW conditions, though none of them did in averaged C vs. H comparative tests ([Supplementary Figure S6a,c](#)).

The four dehydrins showed significantly increased expression levels in drought conditions in most accessions (Wilcoxon tests, [Supplementary Table S8](#); Tukey tests, **Figure 5**, [Supplementary Figure S7](#)). The DE levels were also significantly different among ecotypes, especially within the dry treatment, being highest in warm ecotypes Koz3 (*Bdhn1a*, *Bdhn3*, *Bdhn7*) and Adi10 (*Bdhn2*) and lowest in cold ecotypes ABR2 (*Bdhn1*) and ABR4 (*Bdhn2*, *Bdhn3*, *Bdhn7*) (**Figure 5**, [Supplementary Figure S7](#)). On average drought increased dehydrin expression by about 5.74% in *Bdhn1a*, 39% in *Bdhn2*, 67.8% in *Bdhn3*, and 97.8% in *Bdhn7* compared to well-watered plants ([Supplementary Figure S6b](#)). Overexpression of dehydrins caused by drought stress was significantly correlated between all *Bdhn* gene pairs ([Supplementary Table S9 and Figure S8](#)).

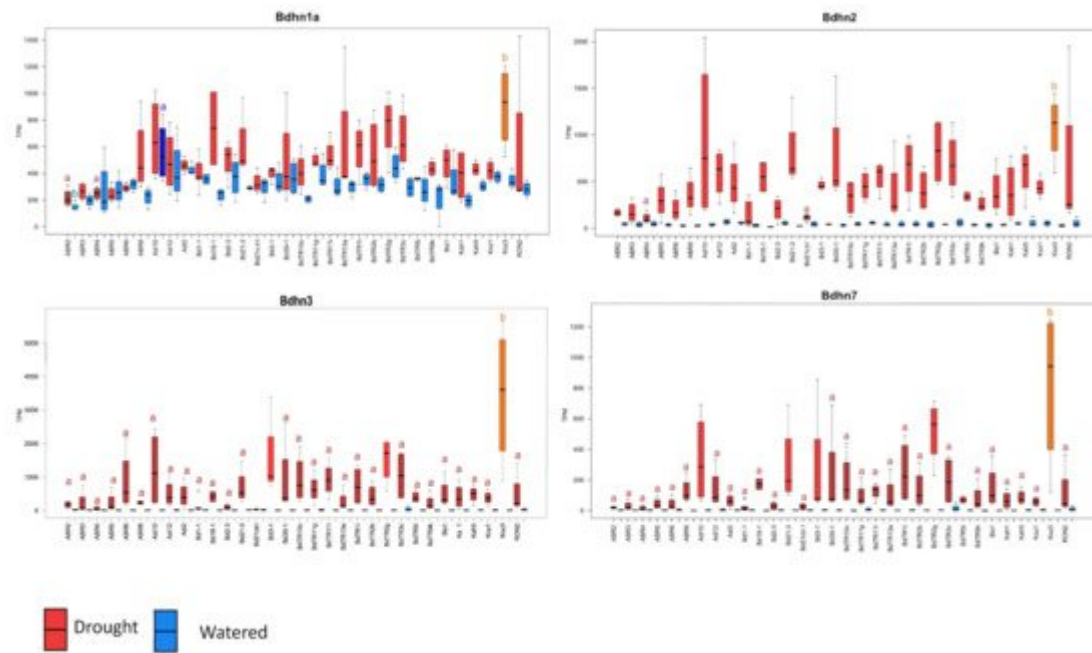


Figure 5. Differentially expressed *Bdhn1a*, *Bdhn2*, *Bdhn3*, and *Bdhn7* dehydrin genes (transcript per million, TPM) in 32 ecotypes of *B. distachyon* under drought (D, red) vs. watered (W, blue) conditions. Different letters in the boxplots indicate significant group differences (Tukey HSD tests) (see also [Supplementary Figure S7](#)).

A *B. distachyon*–*T. aestivum* DE comparative analysis found that the drought-induced *Bdhn1*, *Bdhn2*, *Bdhn3*, and *Bdhn7* genes belong to the same ortholog groups as 15 out of the 16 differentially expressed wheat dehydrin (DHN) genes ([Supplementary Table S10](#)) under natural field drought stress [\[40\]](#) or greenhouse imposed drought stress [\[6\]\[41\]](#). In wheat there is a physical clustering of several dehydrin genes in two gene clusters located in the 5L and 6L groups of wheat chromosomes ([Supplementary Table S10; Supplementary Figure S9](#)). The 6L cluster contains 25 dehydrins and includes nine DHN3 genes and three DHN4 genes (all orthologs to *Bdhn3*), whereas the 5L cluster has 13 DHN38 genes of which six are orthologs to *Bdhn7*. In addition, the DHN11 genes, located in another portion of 6L chromosomes are orthologs to the *Bdhn1* and *Bdhn2* genes. We observed that orthologs from *B. distachyon* and *T. aestivum* tended to show a similar pattern of expression response to soil drying. Specifically, the duplicated *Bdhn1* and *Bdhn2* genes and the DHN11(A1) genes, the *Bdhn7* gene and the duplicated DHN38 (B1, B2) genes, and the *Bdhn3* gene and the duplicated DHN3 (A1, A6, B6, D1, D4, D6, D8, D9) genes were all upregulated in drought treatments ([Supplementary Table S10 and Figure S9; \[40\]](#)).

8. Effects of Drought on Dehydrin Gene Expression and Drought-Response Phenotypic Traits

The potential effect of drought on dehydrin expression levels and on correlated changes of phenotypic and physiological drought-response traits of the plants was evaluated in 32 *B. distachyon* ecotypes. The 12 drought-response phenotypic traits studied (leaf_rwc: relative water content in leaf; leaf_wc: water content in leaf; lma: leaf mass per area; pro: leaf proline content; abvgrd: above ground biomass; blwgrd: below ground biomass; ttlmass: total plant mass; rmr: root mass ratio; delta13c: carbon isotope, a proxy for lifetime integrated WUE; leafc: leaf

carbon content; leafn: leaf nitrogen content; cn: leaf carbon/nitrogen ratio) also showed significant different values in dry vs. watered conditions across ecotypes ([Supplementary Table S11](#)). On average, drought significantly decreased the values of six traits (17.14% in abvgrd, 34.78% in ttlmass, 4% in leaf_rwc, 36.5% in leaf_wc, 12.5% in leafn, 2.8% in WUE) and significantly increased those of five traits (33% in pro, 5.5% in rmr, 2.96% in leafc, 5.71% in lma, 21.4% in cn) compared to watered conditions, but did not significantly affect the blwgrd trait ([Supplementary Figure S10](#)) [2].

Drought-induced effects caused significant positive and negative correlations between the averaged expressed values of the four *Bdhn* genes and changes in most phenotypic trait values ([Supplementary Table S12 and Figure S11](#)). Regression models for independent correlations between the *Bdhn1a*, *Bdhn2*, *Bdhn3*, and *Bdhn7* expressions and the changes in the 12 phenotypic traits showed significant positive correlations for most dehydrin *Bdhn* genes with pro, blwgrd, rmr, WUE, leafc, and cn, negative correlations with leaf_rwc, leaf_wc, and leafn, and non-significant correlations with ttlmass and abvgrd ([Supplementary Figure S11](#)).

9. Phylogenetic Signal of Dehydrin Expression, Phenotypic Trait Changes and Climate Variation in the *Brachypodium distachyon* *Bdhn* Tree

The potential phylogenetic signal of dehydrin expression, phenotypic trait changes, and climate variation was evaluated on both the *B. distachyon* nuclear species tree [37] and the *B. distachyon* dehydrin *Bdhn* tree. None of the dehydrin gene expression values under W or D conditions and few phenotypic and climate traits had significant K or lambda values on the *B. distachyon* nuclear species tree ([Supplementary Table S13a and Figure S12](#)). By contrast, *Bdhn2W*, *Bdhn7W*, and *Bdhn3D* expression values, phenotypic change of rmrW, leafnW, cnW, abwgrdW, leafcD, leafnD, and cnD traits' values and climate niche PCA1 values carried phylogenetic signal (or marginal phylogenetic signal for leaf_rwcD and abvgrdD values) when tested on the dehydrin *Bdhn* tree ([Supplementary Table S13b, Figure 6](#)).

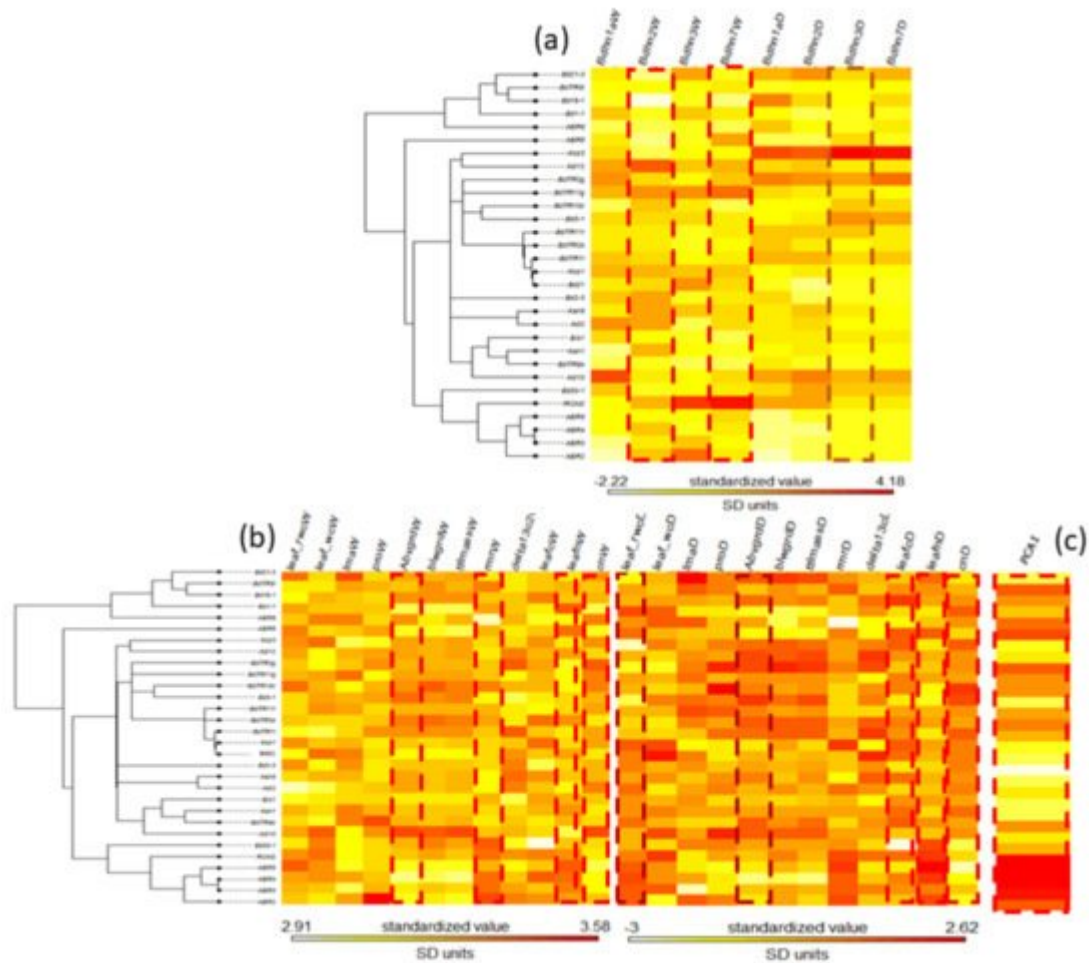


Figure 6. Maximum likelihood *B. distachyon* *Bdhn* tree cladogram showing the relationships of 30 ecotypes. Phyloheatmaps of normalized values for different sets of variables: (a) dehydrin (*Bdhn1*, *Bdhn2*, *Bdhn3*, *Bdhn7*) gene expression values under watered (W) and drought (D) conditions; (b) drought-response phenotypic traits (leaf_rwc: relative water content in leaf; leaf_wc: water content in leaf; lma: leaf mass per area; pro: leaf proline content; abvgrd: above ground biomass; blwgrd: below ground biomass; ttlmass: total plant mass; rmr: root mass ratio; delta13c: carbon isotope, a proxy for lifetime integrated WUE; leafc: leaf carbon content; leafn: leaf nitrogen content; cn: leaf carbon/nitrogen ratio) values under watered (W) and drought (D) conditions; (c) climate niche PC1 values. Traits showing significant phylogenetic signal are highlighted with dotted lines (see [Supplementary Table S13b](#)). Watered (W): soil irrigated to field capacity every second day; Drought (D): soil water content reduced by ~5% each day (during the 10 days experiment).

References

1. Hossain, M.A.; Wani, S.H.; Bhattacharjee, S.; Burritt, D.J.; Tran, L.-S.P. Drought Stress Tolerance in Plants; Springer: Cham, Switzerland, 2016; Volume 2.
2. Des Marais, D.L.; Lasky, J.R.; Verslues, P.E.; Chang, T.Z.; Juenger, T.E. Interactive effects of water limitation and elevated temperature on the physiology, development and fitness of diverse

- accessions of *Brachypodium distachyon*. *New Phytol.* 2017, 214, 132–144.
3. Mahajan, S.; Tuteja, N. Cold, salinity and drought stresses: An overview. *Arch. Biochem. Biophys.* 2005, 444, 139–158.
 4. Hanin, M.; Brini, F.; Ebel, C.; Toda, Y.; Takeda, S.; Masmoudi, K. Plant dehydrins and stress tolerance: Versatile proteins for complex mechanisms. *Plant Signal. Behav.* 2011, 6, 1503–1509.
 5. Tommasini, L.; Svensson, J.T.; Rodriguez, E.M.; Wahid, A.; Malatrasi, M.; Kato, K.; Wanamaker, S.; Resnik, J.; Close, T.J. Dehydrin gene expression provides an indicator of low temperature and drought stress: Transcriptome-based analysis of Barley (*Hordeum vulgare* L.). *Funct. Integr. Genom.* 2008, 8, 387–405.
 6. Reddy, S.K.; Liu, S.; Rudd, J.C.; Xue, Q.; Payton, P.; Finlayson, S.A.; Mahan, J.; Akhunova, A.; Holalu, S.V.; Lu, N. Physiology and transcriptomics of water-deficit stress responses in wheat cultivars TAM 111 and TAM 112. *J. Plant Physiol.* 2014, 171, 1289–1298.
 7. Wang, Y.; Xu, H.; Zhu, H.; Tao, Y.; Zhang, G.; Zhang, L.; Zhang, C.; Zhang, Z.; Ma, Z. Classification and expression diversification of wheat dehydrin genes. *Plant Sci.* 2014, 214, 113–120.
 8. Graether, S.P.; Boddington, K.F. Disorder and function: A review of the dehydrin protein family. *Front. Plant Sci.* 2014, 5, 1–12.
 9. Verma, G.; Dhar, Y.V.; Srivastava, D.; Kidwai, M.; Chauhan, P.S.; Bag, S.K.; Asif, M.H.; Chakrabarty, D. Genome-wide analysis of rice dehydrin gene family: Its evolutionary conservedness and expression pattern in response to PEG induced dehydration stress. *PLoS ONE* 2017, 12, e0176399.
 10. Riley, A.C.; Ashlock, D.A.; Graether, S.P. Evolution of the modular, disordered stress proteins known as dehydrins. *PLoS ONE* 2019, 14, e0211813.
 11. Perdiguero, P.; Collad, C.; Soto, Á. Novel dehydrins lacking complete K-segments in Pinaceae. The exception rather than the rule. *Front. Plant Sci.* 2014, 5, 682.
 12. Goday, A.; Jensen, A.B.; Culiáñez-Macià, F.A.; Albà, M.M.; Figueras, M.; Serratos, J.; Torrent, M.; Pagès, M. The maize abscisic acid-responsive protein Rab17 is located in the nucleus and interacts with nuclear localization signals. *Plant Cell* 1994, 6, 351–360.
 13. Rosales, R.; Romero, I.; Escribano, M.I.; Merodio, C.; Sanchez-Ballesta, M.T. The crucial role of Φ - and K-segments in the in vitro functionality of *Vitis vinifera* dehydrin DHN1a. *Phytochemistry* 2014, 108, 17–25.
 14. Strimbeck, G.R. Hiding in plain sight: The F segment and other conserved features of seed plant SKn dehydrins. *Planta* 2017, 245, 1061–1066.

15. Hennessy, F.; Nicoll, W.S.; Zimmermann, R.; Cheetham, M.E.; Blatch, G.L. Not all J domains are created equal: Implications for the specificity of Hsp40-Hsp70 interactions. *Protein Sci.* 2005, 14, 1697–1709.
16. Malik, A.A.; Veltri, M.; Boddington, K.F.; Singh, K.K.; Graether, S.P. Genome analysis of conserved dehydrin motifs in vascular plants. *Front. Plant Sci.* 2017, 8, 1–18.
17. Kosova, K.; Vıtamvas, P.; Prasil, I.T. Wheat and barley dehydrins under cold, drought, and salinity —What can LEA-II proteins tell us about plant stress response? *Front. Plant Sci.* 2014, 5, 343.
18. Suprunova, T.; Krugman, T.; Fahima, T.; Chen, G.; Shams, I.; Korol, A.; Nevo, E. Differential expression of dehydrin genes in wild barley, *Hordeum spontaneum*, associated with resistance to water deficit. *Plant Cell Environ.* 2004, 27, 1297–1308.
19. Karami, A.; Shahbazi, M.; Niknam, V.; Shobbar, Z.S.; Tafreshi, R.S.; Abedini, R.; Mabood, H.E. Expression analysis of dehydrin multigene family across tolerant and susceptible barley (*Hordeum vulgare* L.) genotypes in response to terminal drought stress. *Acta Physiol. Plant* 2013, 35, 2289–2297.
20. Yu, Z.; Wang, X.; Zhang, L. Structural and functional dynamics of dehydrins: A plant protector protein under abiotic stress. *Int. J. Mol. Sci.* 2018, 19, 3420.
21. Lv, A.; Su, L.; Liu, X.; Xing, Q.; Huang, B.; An, Y.; Zhou, P. Characterization of Dehydrin protein, CdDHN4-L and CdDHN4-S, and their differential protective roles against abiotic stress in vitro. *BMC Plant Biol.* 2018, 18, 299.
22. Liu, Y.; Song, Q.; Li, D.; Yang, X.; Li, D. Multifunctional roles of plant dehydrins in response to environmental stresses. *Front. Plant Sci.* 2017, 8, 1018.
23. Drira, M.; Saibi, W.; Brini, F.; Gargouri, A.; Masmoudi, K.; Hanin, M. The K-segments of the wheat dehydrin DHN-5 are essential for the protection of lactate dehydrogenase and β -glucosidase activities in vitro. *Mol. Biotechnol.* 2013, 54, 643–650.
24. Xing, X.; Liu, Y.; Kong, X.; Liu, Y.; Li, D. Overexpression of a maize dehydrin gene, ZmDHN2b, in tobacco enhances tolerance to low temperature. *Plant Growth Regul.* 2011, 65, 109–118.
25. Xu, J.; Zhang, Y.X.; Wei, W.; Han, L.; Guan, Z.Q.; Wang, Z.; Chai, T.Y. BjDHNs confer heavy-metal tolerance in plants. *Mol. Biotechnol.* 2008, 38, 91–98.
26. Hara, M.; Kondo, M.; Kato, T. A KS-type dehydrin and its related domains reduce Cu-promoted radical generation and the histidine residues contribute to the radical-reducing activities. *J. Exp. Bot.* 2013, 64, 1615–1624.
27. Koag, M.C.; Fenton, R.D.; Wilkens, S.; Close, T.J. The binding of maize DHN1 to lipid vesicles. Gain of structure and lipid specificity. *Plant Physiol.* 2003, 131, 309–316.

28. Hughes, S.L.; Schart, V.; Malcolmson, J.; Hogarth, K.A.; Martynowicz, D.M.; Tralman-Baker, E.; Patel, S.N.; Graether, S.P. The importance of size and disorder in the cryoprotective effects of dehydrins. *Plant Physiol.* 2013, 163, 1376–1386.
29. Scholthof, K.-B.G.; Irigoyen, S.; Catalán, P.; Mandadi, K.K. Brachypodium: A monocot grass model system for plant biology. *Plant Cell* 2018, 30, 1673–1694.
30. Gordon, S.P.; Contreras-Moreira, B.; Levy, J.J.; Djamei, A.; Czedik-Eysenberg, A.; Tartaglio, V.S.; Session, A.; Martin, J.; Cartwright, A.; Katz, A.; et al. Gradual polyploid genome evolution revealed by pan-genomic analysis of *Brachypodium hybridum* and its diploid progenitors. *Nat. Commun.* 2020, 11, 3670.
31. Steinwand, M.A.; Young, H.A.; Bragg, J.N.; Tobias, C.M.; Vogel, J.P. *Brachypodium sylvaticum*, a Model for Perennial Grasses: Transformation and Inbred Line Development. *PLoS ONE* 2013, 8, e75180.
32. Lee, K.; Kang, H. Emerging roles of RNA-binding proteins in plant growth, development, and stress responses. *Mol. Cells* 2016, 39, 179–185.
33. Ryu, H.; Cho, Y.G. Plant hormones in salt stress tolerance. *J. Plant Biol.* 2015, 58, 147–155.
34. Yoon, J.S.; Kim, J.Y.; Lee, M.B.; Seo, Y.W. Over-expression of the *Brachypodium* ASR gene, BdASR4, enhances drought tolerance in *Brachypodium distachyon*. *Plant Cell Rep.* 2019, 38, 1109–1125.
35. Filiz, E.; Ozyigit, I.I.; Tombuloglu, H.; Koc, I. In silico comparative analysis of LEA (Late Embryogenesis Abundant) proteins in *Brachypodium distachyon* L. *Plant Omi. J.* 2013, 6, 433–440.
36. Rodríguez, E.M.; Svensson, J.T.; Malatrasi, M.; Choi, D.W.; Close, T.J. Barley Dhn13 encodes a KS-type dehydrin with constitutive and stress responsive expression. *Theor. Appl. Genet.* 2005, 110, 852–858.
37. Gordon, S.P.; Contreras-Moreira, B.; Woods, D.P.; Des Marais, D.L.; Burgess, D.; Shu, S.; Stritt, C.; Roulin, A.; Schackwitz, W.; Tyler, L.; et al. Extensive gene content variation in the *Brachypodium distachyon* pan-genome correlates with population structure. *Nat. Commun.* 2017, 8, 2184.
38. Sancho, R.; Cantalapiedra, C.P.; López-Alvarez, D.; Gordon, S.P.; Vogel, J.P.; Catalán, P.; Contreras-Moreira, B. Comparative plastome genomics and phylogenomics of *Brachypodium*: Flowering time signatures, introgression and recombination in recently diverged ecotypes. *New Phytol.* 2018, 218, 1631–1644.
39. Sancho, R.; Catalán, P.; Contreras-Moreira, B.; Juenger, T.E.; Des Marais, D.L. Patterns of gene co-expression under water-deficit treatments and pan-genome occupancy in *Brachypodium distachyon*. *bioRxiv* 2021.

40. Gálvez, S.; Mérida-García, R.; Camino, C.; Borrill, P.; Abrouk, M.; Ramírez-González, R.H.; Biyiklioglu, S.; Amil-Ruiz, F.; Dorado, G.; Budak, H.; et al. Hotspots in the genomic architecture of field drought responses in wheat as breeding targets. *Funct. Integr. Genom.* 2019, *19*, 295–309.
41. Chu, C.; Wang, S.; Paetzold, L.; Wang, Z.; Hui, K.; Rudd, J.C.; Xue, Q.; Ibrahim, A.M.H.; Metz, R.; Johnson, C.D.; et al. RNA-seq analysis reveals different drought tolerance mechanisms in two broadly adapted wheat cultivars 'TAM 111' and 'TAM 112'. *Sci. Rep.* 2021, *11*, 4301.

Retrieved from <https://www.encyclopedia.pub/entry/history/show/40388>